Astron. & Astrophys. 30, 305—315 (1974)

The Radio Structure of Quasars. II

J. F. C. Wardle* and G. K. Miley**
National Radio Astronomy Observatory***, Green Bank, West Virigina

Received September 6, 1973

Summary. The structures of thirty nine quasars with known redshifts have been studied with the NRAO interferometer at wavelengths of 11.1 and 3.7 cm. At the shorter wavelength, the angular resolution is about one arcsec. Twelve sources were unresolved, five sources were slightly resolved, and structures have been derived at both frequencies for the remainder. Nearly half of the well resolved sources were found to have more than two components. The "largest angular size-redshift" diagram is extended to 166 quasars, and is interpreted in terms of the "ram pressure" model for the containment of extended radio sources. It is shown that for the largest quasars at large redshifts there is a serious conflict between their radiative and dynamic lifetimes.

Key words: quasars – radio structure – cosmology – radio source models

I. Introduction

Macdonald and Miley (1971) (Paper I) investigated the angular structure of 79 quasars with known redshifts, with the NRAO interferometer at a wavelength of 11.1 cm. Together with previous work, mainly by Hogg (1969), this brought the total number of quasars with known redshifts and structural information to 127. The results up to 1971 have been reviewed by Miley (1971).

Since then, redshifts have been determined for 39 more (Schmidt, Wills, personal communications). Most of these are faint sources from the 4 C catalog, and many have quite large redshifts, including the source 0805+04 ($z=2.877$, Wills and Lynds, 1970). Also, the NRAO interferometer has been converted to operate simultaneously at wavelengths of 11.1 cm and 3.7 cm. We have, therefore, observed the structures of the 39 quasars with recently determined redshifts at both wavelengths, and reobserved at 3.7 cm wavelengths 69 of the quasars observed in Paper I in order to obtain detailed spectral index information for these sources. This latter group of sources will be discussed in Paper III (Miley and Wardle, in preparation). Here we report the observations of the 39 quasars with recently determined redshifts. A preliminary account of this work was given by Wardle and Miley (1971).

II. The Observations

The NRAO three-element interferometer (Hogg *et al.*, 1969) consists of three 85 foot paraboloids mounted equatorially. Sources with positive declinations can be observed between hour angles $\pm 5^h40^m$, and those with negative declinations between $\pm 4^h35^m$. Simultaneous observations at 2695 and 8085 MHz were made with six double-sideband interferometers, each with a bandwidth of 30 MHz. The feeds were left hand circularly polarized at 2695 MHz, and right hand circularly polarized at 8085 MHz. The rms noise after 30 s integration was about .05 fu at 2695 MHz and .07 fu at 8085 MHz. [One flux unit (fu) $= 10^{-26}$ W Hz^{-1} m^{-2}.]

The observations were made in two stages. During both sessions the lengths of the three baselines were 900 m, 1800 m and 2700 m. In June, 1970, each source was observed for a 15 min period once every hour throughout the available range of hour angles. A preliminary analysis of the data was made to select those sources whose frings amplitude varied appreciably with hour angle, indicating that they were well resolved by the interforemeter. These sources were reobserved in September 1970, when they were tracked throughout the available hour angle range.

The calibration technique was the same for both sessions. A "calibration source", whose position and flux density was well known, was observed every hour for 15 min. These observations were used to determine both the baseline parameters and the day to day gain and phase-centers of the interferometers. The calibration sources used were 3 C 48, CTA 21, 0237–23, 3 C 147, 1127–14, 3 C 286, 3 C 287 and 3 C 309.1. The positions of these sources were taken from Wade (1970). Their flux densities at 2695 MHz were taken from Kellermann *et al.* (1968), and their flux densities at

* Present address: Brandeis University, Waltham, Massachusetts.
** Present address: Sterrewacht, Leiden, Netherlands
*** Operated by Associated Universities, Inc., under contract with the National Science Foundation.

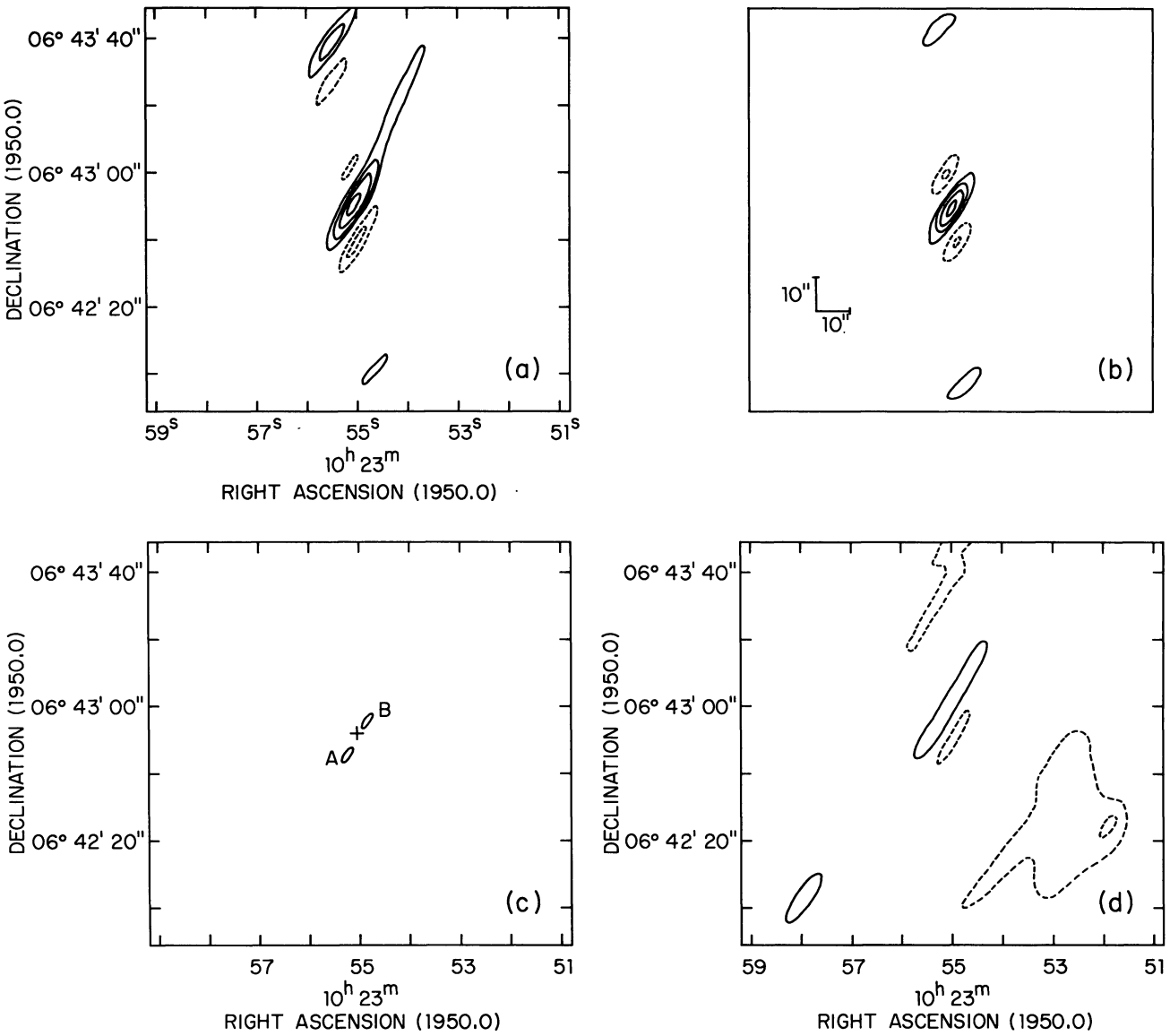

Fig. 1. a) Synthesized map of 1023+06 at 2695 MHz. The contour interval is 20% of the peak brightness, and the lowest contour level has been omitted for clarity. Broken lines refer to negative contour levels. b) Synthesized beam. The contour levels are as in (a). c) Adopted model for 1023+06. The parameters of the model are given in Table 3. The cross marks the position of the optical object. d) "Difference map" made by subtracting the adopted model from the data (see text). The lowest contour level is 5% of the peak brightness in (a). The contour interval is 5%

8085 MHz were taken from spectra compiled by Kellermann (personal communication).

III. The Analysis

The sources have been divided into three groups: (a) sources whose fringe amplitude did not vary significantly at any baseline; (b) slightly resolved sources for which structures could not be derived; (c) well resolved sources. For the unresolved sources, an upper limit for the angular size in the direction of maximum resolution (position angle $\sim 70°$) of about one arcsec can be assigned. In other position angles the limit must be increased somewhat. For the slightly resolved sources, an equivalent gaussian diameter can be calculated together with the position angle of elongation. Since sources are usually found to consist of more than one component, rather than a single component with a gaussian brightness distribution, the angular sizes in Table 2 are given as upper limits.

For the well resolved sources, a variety of techniques were used to determine their structures. First, maps of the brightness distributions were produced by the Fourier inversion method described by Hogg *et al.* (1969). Due to the rather limited coverage of the $u-v$ plane, the maps were distorted by the high side lobe level of the synthesized beam. However, compari-

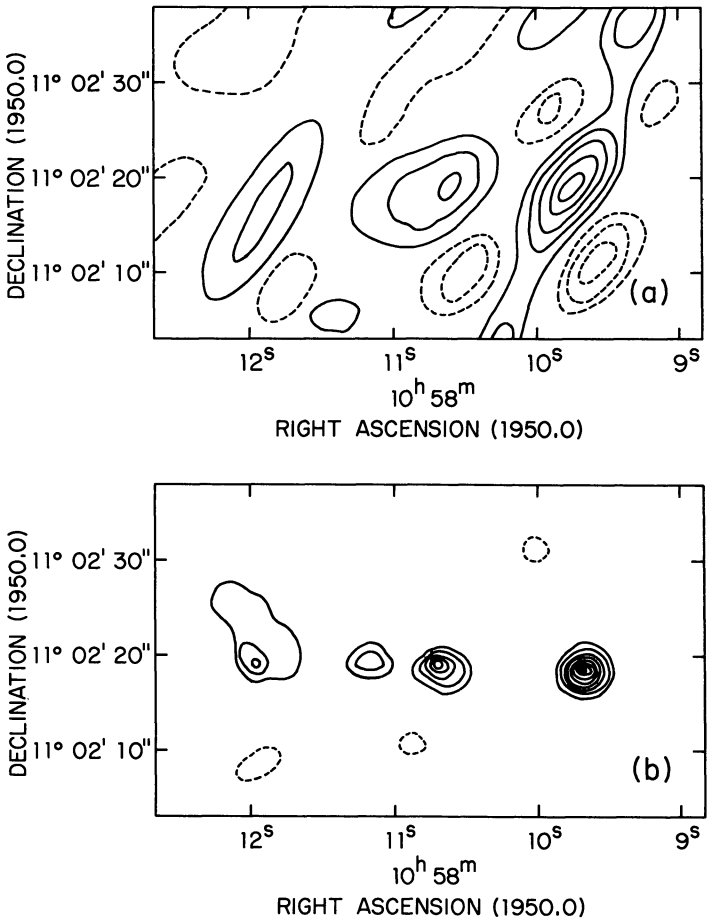

Fig. 2. a) Synthesized map of 1058+11 at 2695 MHz. The lowest contour and the contour interval are 20% of the peak brightness. Broken lines refer to negative contour levels. b) "Clean" map of 1058+11, after using the procedure outlined in the text. The map has been convolved with a circular gaussian beam with a half power width of 3 arcsec. The lowest contour level and the contour interval are 10% of the peak brightness. The cross marks the position of the optical object, and the parameters of the components are given in Table 3

son with the derived beam shape usually revealed the main features of the structure. From the maps and from the raw fringe visibilities, a model of each source was derived. This was then used as input to an iterative model fitting program, which compared the fringe amplitude calculated from the model with the observed fringe amplitude at each point in the $u-v$ plane. The parameters of the model were adjusted to minimize the residuals in the least squares sense. The "best fitting" model so derived was checked by producing a map by Fourier inversion of the vector difference between the observed fringe amplitude and the fringe amplitude calculated from the model. The model was considered satisfactory if (a) it accounted for at least 90% of the total flux of the source, and (b) the peak brightness temperature in the "difference" map was less than 10% of the peak brightness temperatures in the original map. Since most of the sources were rather weak, these criteria are quite severe.

This procedure worked particularly well for sources with reasonably compact components whose brightness distributions could be approximated reasonably well by elliptical gaussian functions. An example is given in Fig. 1 of the Fourier inversion map, the synthesized beam and the difference map for 1023+06. The derived model for this source is given in Table 3.

For complex sources with extended of asymmetric components, a data restoration technique developed by Hogbom (1973) was also used. A map of the brightness distribution and of the synthesized beam was produced by Fourier inversion in the usual way. The response to a "point" source (i.e. the synthesized beam) was then subtracted from the brightness point in the map. This procedure was repeated until no significant structure remained in the map. Thus the source was approximated by a large number of "point" sources. A smoothed brightness distribution for the source was then reconstructed by convolving the "point" sources with a circular gaussian beam shape of roughly the same area as the original synthesized beam. This technique, often referred to as "cleaning" the maps, proved useful in analysing the extended low surface brightness components and the complex sources. An example is given in Fig. 2 for the source 1058+11.

Because of the limited coverage in the $u-v$ plane, it was not possible to determine the brightness distributions in great detail. However, as in Paper I, the purpose of this work was to determine the main features of the structure of many sources rather than detailed information on only a few.

The accuracy of the derived structure parameters is difficult to assess. The sensitivity of the model fitting procedures to variations in the parameters depends on the structure of the source and on the sampling in the $u-v$ plane, and the derived parameters are interdependent in a complicated way. In order to reduce the total number of parameters to be solved for, it was assumed that each component was oriented parallel to the line joining the components. This is generally a reasonable approximation (see, for example, Macdonald *et al.*, 1968). In Table 3 it is believed that the relative positions are accurate to better than a second of arc, the component sizes are accurate to about one second of arc, and the component flux densities have errors of about 20% or .02 fu, whichever is greater.

IV. The Results

In Table 1 the results for the unresolved sources are given. The first column gives the name of the source in the usual Parkes notation. Sources that are listed in the Parkes surveys are prefaced by a P. The second column gives the name of the source in the 4 C catalog, and the third column lists other well known names of the source. Columns five and six give the integrated flux density of the source at 2695 MHz, and the reference to the measurement. The references are as follows:

1. Merkelijn, J.K. 1969, *Australian J. Phys.* **22**, 237
2. Wills, D., Bolton, J.G. 1969, *Australian J. Phys.* **22**, 775
3. Wall, J.V., Shimmins, A.J., Merkelijn, J.K. 1971, *Australian J. Phys. Astrophys. Suppl.* **19**,

Table 1. The unresolved sources

Source	4 C	Other	Total flux density at 2695 MHz (fu)	Ref.	Observed fringe amplitude at 2695 MHz (fu)	Observed fringe amplitude at 8085 MHz (fu)	α_{2695}^{8085}
P 0424−13		NRAO 178	0.60 ± .04	1	0.55 ± .03	0.15 ± .03	−1.18
1022+19	19.34	OL 136	0.56 ± .04	2	0.43 ± .03	0.60 ± .04	+0.30
1038 06	06.41		1.74 ± .12	2	1.75 ± .08	1.40 ± .10	−0.20
P 1335+023			0.104 ± .011	3	0.12 ± .02	0.09 ± .02	−0.26
1502+60	60.19	3 C 311 DA 375 NRAO 467	0.80 ± .04	4	0.81 ± .04	0.30 ± .03	−0.90
1611+34		DA 406	2.98 ± .15	15	2.58 ± .10	2.31 ± .12	−0.10
P 1801+01		DW 1801+01	0.90 ± .06	5	0.79 ± .03	0.92 ± .06	+0.14
P 2144−17			0.60 ± .04	5	0.57 ± .03	0.23 ± .03	−0.83
P 2149+21	21.59	DA 565	0.50 ± .04	6	0.55 ± .04	0.26 ± .03	−0.68
2156+29	29.64	CTD 133 DW 2156+29			0.72 ± .03	0.33 ± .03	−0.71
2201+31	31.63	B 2.2201+31 A	2.01 ± .10	15	1.66 ± .09	3.06 ± .15	+0.56
P 2223+21		DA 580	1.40 ± .11	6	1.91 ± .08	~1.1	~ .50

1424−13 Spectrum has a maximum at about 750 MHz.
1022+19 Low frequency spectral index is −.67. May be variable.
1038+06 Complex, fairly flat spectrum.
1335+023 No other spectral information.
1502+60 Flux density at 4995 MHz is 0.47 ± .04 fu (11). Straight spectrum.
1611+34 Kellermann *et al.* (1971) find that the source is unresolved at a wavelength of 6 cm ($\theta \lesssim 0.0008$ arcsec). At a wavelength of 18 cm, there is a larger component present which contains half of the total flux and is completely resolved with a baseline of $1.66 \times 10^7\ \lambda$, ($\theta \gtrsim 0.01$ arcsec). The spectrum is fairly flat at high frequencies and probably opaque below 408 MHz, (8, 12, 14).
1801+01 Complex spectrum. Flux densities at 5009 MHz; 0.33 ± .02 fu (9), 6630 MHz: 0.69 ± .12 fu (13), 10700: 0.72 ± .20 fu (13). Spectrum has a maximum at about 408 MHz. May be variable.
2144−17 Convex Spectrum. Flux density at 5009 MHz is 0.33 ± .02 fu (9).
2149+21 Fairly straight spectrum. Mean spectral index is −.86.
2156+29 Straight spectrum. Mean spectral index is −.76.
2201+31 Spectrum has a minimum near 2000 MHz. Low frequency spectral index is 0.36. May be variable.
2223+21 Definitely variable at 8085 MHz. The observed flux densities at this frequency were 1.19 ± .04 fu in June 1970 and 0.99 ± .04 fu in September 1970. This is a remarkably rapid variation in the 2695 MHz fringe amplitude between these dates. The epoch of the total flux density measurement at 2695 MHz (5) was 1967.3. The flux density at 5009 MHz has been measured to be 1.35 ± .03 fu (9, epoch 1968.5), and 1.51 ± .07 fu (15, epoch 1970.4). The low frequency spectrum is uncertain, but it is probably fairly flat.

4. Kellermann, K. I., Pauliny-Toth, I. I. K., Tyler, W. C. 1968, *Astrophys. J.* **73**, 298
5. Staff of the Division of Radiophysics, CSIRO 1969, *Australian J. Phys. Astrophys. Suppl.* **7**
6. Shimmins, A. J., Day, G. A. 1968, *Australian J. Phys.* **21**, 377
7. Olsen, E. T. 1967, *Astrophys. J.* **72**, 738
8. Davis, M. M., private communication
9. Shimmins, A. J., Manchester, R. N., Harris, B. J. 1969, *Australian J. Phys. Astrophys. Suppl.* **8**
10. Kellermann, K. I., private communication
11. Pauliny-Toth, I. I. K., Kellermann, K. I. 1968, *Astrophys. J.* **73**, 953
12. Grueff, G 1971, *Astrophys. J.* **76**, 530
13. Bell, M. B., Seaquist, E. R., Braun, L. D. 1971, *Astrophys. J.* **76**, 524
14. Bridle, A. 1969, *Nature* **221**, 348
15. Witzel, A., Veron, P., Veron, M. P. 1971, *Astron. & Astrophys.* **11**, 171
16. Galt, J. A., Kennedy, J. E. D. 1968, *Astrophys. J.* **73**, 135

The last three columns give the measured fringe amplitude at 2695 MHz and 8085 MHz and the corresponding spectral index between these two frequencies. The spectral index is defined in the sense of $S \propto \nu^{\alpha}$, where S is the flux density measured at a frequency ν, and α is the spectral index. Notes on the spectra of these sources, and other information on their structure are given below Table 1. The source 2223+21 was found to have varied appreciably in flux density at 8085 MHz between the two periods of observation. This is the only source in Table 1 that was observed in both sessions, so rapid variability cannot be ruled out for the other sources.

The results for the slightly resolved sources are given in Table 2. The first six columns are the same as for Table 1, all the sources being essentially unresolved at 2695 MHz. Columns seven and eight give the maximum and minimum fringe amplitudes observed at 8085 MHz. Columns nine and ten give the largest angular size and the position angle of elongation. For the reasons given earlier these sizes should be considered upper limits. Column eleven gives the observed spectral index between 8085 MHz and 2695 MHz. Additional information on the sources is given in the notes below Table 2.

Table 3 gives the results for the well-resolved sources. The meaning of the columns is:

1–5 Same as for Tables 1 and 2.

6, 7 The maximum observed fringe amplitudes at 2695 MHz and 8085 MHz. If the source components are reasonably compact, these values should be close to the integrated flux density of the source.

8 The morphological classification of the radio structure: D–Double, with two distinctly separated regions of radio emission. We have not attempted to distinguish D 1 and D 2 type doubles (see Paper 1).
T–Triple. C–Complex, with more than three distinct components. H–The subscript H indicates that the maximum observed fringe amplitude is significantly less than the integrated flux density. There is probably large scale structure present (> 30 arcsec) which is completely resolved, even at our lowest resolution.

9, 10 For sources with two or more components, these give the length and orientation of a line joining the two most widely separated components.

11–17 The parameters of the individual components. Columns 12 and 13 give the positions of components relative to the most intense component. Columns 14 and 15 give the angular size of the components in two directions, parallel and perpendicular to the major axis of the source respectively. These should be accepted with some caution due to the limited coverage of the $u-v$ plane. Because of the large difference in resolution between 2695 MHz and 8085 MHz, the component sizes could usually be determined at only one frequency. Columns 16 and 17 give the flux densities of the components at both frequencies.

Additional information on these sources is given in notes below Table 3.

Table 2. The slightly resolved sources

Source	4C	Other	Total flux density at 2695 MHz (fu)	Ref.	Observed fringe amplitude 2695 MHz (fu)	Maximum observed fringe amplitude 8085 MHz (fu)	Minimum observed fringe amplitude 8085 MHz (fu)	Angular size (arcsec)	Position angle of elongation (degrees)	α_{2695}^{8085}
0202+31		DW 0202+31 B 2.0202+31	0.70±.07	8	0.81±.03	1.49±.08	1.28±.08	≲4	160	+0.55
0805+04	05.34		0.46±.03	2	0.42±.03	0.29±.03	0.21±.02	≲7	135	−0.34
0843+13	13.39		0.28±.02	2	0.23±.02	0.14±.02	0.08±.02	≲4	110	−0.45
1210+13	13.46	ON 119	0.95±.06	2	0.95±.05	0.50±.04	0.40±.04	≲4	110	−0.58
1632+39	39.46				0.57±.03	0.29±.03	0.23±.03	≲3	50	−0.62

0202+31 Flux densities at 5000 MHz: 0.87±.04 fu (12), 15000 MHz: 0.9±.1 fu (8), 31500 MHz: 1.2±.1 fu (10). Fairly flat spectrum at all wavelengths. Probably variable.
0805+04 This source has the second largest known redshift, ($z = 2.877$, Lynds and Wills, 1970). Spectrum may be concave.
1843+13 Spectrum may be concave.
1210+13 Straight spectrum. Mean spectral index is −.54.
1632+39 Flux density at 1417 MHz is 1.0±.1 (7). Probably straight spectrum.

Table 3. The resolved sources

Source	4C	Other	Total flux density 2695 MHz (fu)	Ref.	Max observed fringe amplitude 2695 MHz (fu)	Max observed fringe amplitude 8085 MHz (fu)	Morphological type	Largest angular size (arcsec)	Position angle (degrees)	Component	$\Delta\alpha$ (arcsec)	$\Delta\delta$ (arcsec)	ω (arcsec)	ω (arcsec)	Flux density 2695 MHz (fu)	Flux density 8085 MHz (fu)
P 0814+22	22.20	3 C 179	0.71±.04	4	0.75±.04	0.27±.04	C	24	169	A			1.0	1.0	0.47	0.17
		NRAO 287	0.80±.06	6						B	0.4 W	6.7 N	4.0	2.5	0.06	0.04
		OJ 225								C	0.3 W	17.2 N	3.5	3.0	0.04	0.01
										D	4.6 W	23.7 N	1.0	2.0	0.13	0.06
0844+31	31.32	B 2.0844+31 B			0.15±.02	0.07±.02	T_H	81	153	A			≳ 5	≳ 5	(0.07)	
		OJ 374								B	38 W	42 N	≳ 5	≳ 5	(0.04)	
										C	37 W	72 N	≳ 5	≳ 5	(0.04)	
P 0846±10	09.31		0.29±.02	2	0.13±.02	+0.04	D_H	57	41	A			≳15	≳15	0.09	< .04
			0.50±.03	5						B	38 W	43 S	≳15	≳15	0.07	< .04
0911+05	05.38		0.26±.02	2	0.13±.03	0.09±.02	D_H	55	4	A			~ 7	~ 7	0.10	(.05)
										B	4.0 W	54.7 S	~ 3	~ 3	0.04	(.02)
0926+11	11.32		0.26±.02	2	0.28±.03	0.08±.02	D	6.3	47	A			< 2.0	< 2.0	0.19	0.07
										B	4.3 W	4.3 S	(< 2.0)	(< 2.0)	0.08	0.02
0952+09	09.35		0.25±.02	2	0.26±.02	0.10±.02	D	10.5	128	A			4.0	4.0	0.15	0.06
										B	8.2 W	6.5 N	4.5	3.5	0.11	0.04
P 1023+06	06.40	3 C 243	0.34±.03	2	0.39±.02	0.13±.02	D	11.4	149	A			5.5	1.5	0.21	0.08
		NRAO 355	0.35±.04	4						B	5.8 W	9.8 N	5.5	1.5	0.17	0.05
		MSH 10+006														
1046+05	05.46		0.16±.02	2	0.19±.02	0.08±.02	D	9.7	103	A			1.0	1.0	0.11	0.04
										B	9.4 W	2.2 N	1.0	1.0	0.08	0.03
1047+09	09.37		0.22±.02	2	0.22±.02	0.08±.02	D	66	117	A			3.0	3.0	0.18	0.06
										B	59 W	30.5 N	4.5	4.0	0.04	0.02
1058+11	10.30		0.38±.03	2	0.38±.03	0.08±.02	C	34.2	89	A			4.0	3.5	0.11	0.03
										B	15 E	0.5 N	3.5	3.0	0.07	0.01
										C	22 E	0.9 N	3.5	3.0	0.04	0.01
										D	34.2 E	0.8 N	6.5	6.0	0.07	0.02
1104+16	16.30	OM 109	0.68±.05	2	0.60±.03	0.60±.04	D	6.8	129	A			1.0	1.0	(0.50)	0.50
										B	5.3 W	4.3 N	1.0	1.0	(0.10)	0.10
1130+10	10.33		0.47±.03	2	0.55±.04	0.27±.03	S	4.0	109	A			4.0	2.5	0.55	0.27
1203+10	10.34		0.22±.02	2	0.22±.03	0.08±.02	S_H	~20	~ 90	A			2.0	2.0	0.18	0.08
1221+18	18.34	ON 135	0.26±.02	2	0.25±.02	0.09±.02	T	23.0	127	A			4.0	3.0	0.12	0.04
										B	11.7 E	7.1 S	2.0	1.0	0.04	0.03
										C	18.4 E	13.8 S	5.0	3.0	0.09	0.03
P 1318+11	11.45	DA 342	1.20±.07	5	1.24±.08	0.42±.05	D	5.3	27	A			1.0	1.0	0.98	0.34
		OP 131	1.38±.10	1						B	2.4 E	4.7 N	2.0	1.0	0.28	0.08
P 1423+24	24.31	CTD 87	1.00±.08	6	0.78±.05	0.28±.03	T	19.8	22	A			2.0	1.0	0.40	0.14
		OQ 236								B	1.6 W	11.2 S	4.0	3.0	0.14	0.09
										C	7.3 W	18.4 S	2.0	2.0	0.26	0.11
1425+26		Ton 202	0.23±.02	8	0.08±.02	0.07±.02	S_H	>60		A			(< 1)	(< 1)	0.08	0.07
P 1623+26	26.48		0.50±.04	6	0.40±.03	0.10±.03	T	5.6	33	A			2.0	1.0	0.14	0.04
										B	1.1 E	1.4 N	1.0	1.0	0.06	0.02
										C	3.1 E	4.7 N	2.5	1.0	0.13	0.04
1628+36	36.28				0.28±.03	0.09±.02	T	15.7	43	A			3.0	1.5	0.13	0.04
										B	6.1 W	7.3 S	3.5	1.0	0.07	0.03
										C	10.8 W	11.4 S	1.5	1.5	0.08	0.03
See notes to Table 3																
P 2005−04	−04.76	3 C 407	0.64±.04	4	0.54±.03	0.28±.03	C	22	40	A			1.0	< 1.0		0.19
		NRAO 623	0.60±.04	5						B	1.3 W	3.6 N	2.0	1.5	0.85	0.04
		MSH 20−001								C	2.6 E	3.5 S	2.0	< 1.0		0.04
P 2325+26	27.52	3 C 463	0.80±.04	4	0.85±.05	0.28±.03	T	8.1	151	A			1.0	< 1.0	0.31	0.13
		CTD 140	0.60±.04	5						B	4.5 E	3.8 N	< 1.0	1.5	0.09	0.03
		NRAO 713														
2353+28	28.59				0.40±.05	0.15±.03	D	5.9	50							

0814+22 Flux density at 5009 MHz is 0.45 ± .02 fu (9). The spectrum is straight between 430 MHz and 8085 MHz with a spectral index of −.83. Harris and Hardbeck (1969) find scintillation at 430 MHz with a visibility of 60%. This is probably due to component A.

0844+31 Almost completely resolved and the source parameters are very uncertain. Below 1400 MHz the spectrum is straight with a spectral index of −.72. Extrapolating this to higher frequencies the total flux densities should be about 0.94 fu at 2695 MHz and 0.42 fu at 8085 MHz. Olsen (1967) detected large scale structure at 1417 MHz using an interferometer with a baseline of 1160 λ. The correct optical identification is not clear; component A appears to be associated with an E galaxy and components B and C lie on either side of the quasi-stellar object (see Olsen, 1970).

1846+10 Almost completely resolved. Harris and Hardbeck (1969) find no scintillation at 430 MHz (visibility <40%). The spectrum is rather uncertain, but the spectral index is about −.8.

0911+05 Well resolved. The low frequency spectral index is about −.8.

0926+11 Spectral index is −.99. Parameters for the weaker component are rather uncertain.

0952+09 Straight spectrum. Spectral index is −.86.

1023+06 Unresolved (15 arcsec) in an E − W direction at 1425 MHz, (Fomalont, 1968). Harris and Hardbeck (1969) find scintillation at 430 MHz with a visibility of 20%. The spectrum is straight and steep, with a spectral index of −1.32.

1046+05 Spectrum is probably straight with a spectral index of −.68.

1047+09 Straight spectrum. Spectral index is +.95.

1058+11 The spectrum is straight with a spectral index of −.95. At 2695 MHz there is .07 fu contained in an extended bridge between the inner components. This is completely resolved at 8085 MHz.

1104+16 Spectral index is −.85 at low frequencies and flat above 1400 MHz. The data are poor at 2695 MHz and further observations are needed at both frequencies. There is a source visible at 2695 MHz about 15″ S and 7″ W of component.

1130+10 Straight spectrum with a spectral index of −.77. May be more complicated than a single component: two components with a strong bridge would also fit the data.

1203+10 Straight spectrum with a spectral index of −.93. At 2695 MHz there is .04 fu in a halo which is at least 20 arcsec in extent and elongated in position angle 90°. This component is completely resolved at 8085 MHz.

1221+18 Straight spectrum. Spectral index is −.93.

1318+11 Fomalont (1968) found the source was smaller than 15 arcsec in an E − W direction at 1425 MHz. Harris and Hardbeck (1969) found scintillation with a visibility of 30% at 430 MHz. The spectrum is convex with a break at about 430 MHz. The low frequency spectral index is −.64, and the high frequency spectral index is −.94. The flux densities at 5009 MHz are .83 ± .08 fu (15) and .75 ± .03 fu (9). The flux density at 3200 MHz is 1.1 ± .1 fu (16).

1423+24 Flux density at 5009 MHz is .51 ± .03 fu (9). Straight spectrum with a spectral index of −.90.

1425+26 This source has been discussed by Greenstein and Oke (1970). Flux density at 4995 MHz is .16 ± .02 (8). It appears to have a fairly straight spectrum with a spectral index of −.59. The fringe amplitude does not vary significantly with hour angle, but the data are noisy. There is a large component present which is completely resolved at both frequencies (≧ 1 arcmin).

1623+26 There is a confusing source nearby which affexts the 2695 MHz data. The spectrum is convex with a break at about 850 MHz. Above the break the spectral index is −1.27.

1628+36 Straight spectrum with a spectral index of −1.00.

2005−04 This source was well resolved at both frequencies and further observations are needed to establish its structure. The low frequency spectral index is −1.02, and the spectrum flattens above 2695 MHz. The structure appears to consist essentially of two components separated by about 22 arcsec in position angle 40° placed symmetrically about a third compact components which is optically thick at 2695 MHz. At 8085 MHz the central component has a flux density of about 0.14 fu and the outer components both have flux densities of about .07 fu. There may also be extended structure to the northo-west of the compact central component.

2325+26 Straight spectrum with a spectral index of −.91.

2353+28 Straight spectrum. The spectral index is −.75.

V. Discussion

The general features of the radio structure of quasars have been discussed from a morphological point of view by Miley (1971). Although the results presented here agree with his conclusions, we shall add some further comments.

The 39 sources have been divided into three groups according to their angular size-unresolved, slightly resolved, and well-resolved sources. The numbers of sources falling into each group are shown in Table 4, together with the corresponding percentages, their median redshifts and their median spectral indices.

Table 4

	Number	%	⟨z⟩	⟨α⟩
Unresolved	12	31	1.1	−0.3
Slightly resolved	5	13	1.5	−0.5
Resolved	22	56	.8	−0.9

More than half of the radio sources associated with quasars are extended, usually consisting of two or more well-separated and relatively compact components. This type of source appears to be indistinguishable in its radio properties from the strong radio galaxies (cf. Mackay, 1971; Hogg, 1969). In Paper I, the percentage of well resolved sources was slightly lower (46%) due to the poorer resolution of the interferometer at 2695 MHz.

The median values of the redshift and the spectral index for the slightly resolved sources have large statistical errors, since there are only five sources in this group. However, the differences in the median redshift and the median spectral index between the resolved sources are highly significant. The correlation between angular size and redshift was first noted by Miley in 1968, and will be discussed in detail in Section VI. The correlation between angular size and spectral index

has been noted by many authors (e.g. Hogg, 1969), and is probably caused by the dependence of the mean opacity of a source on its compactness (van der Laan, 1969).

Over one third (eight out of twenty-two) of the resolved sources consist of more than two components, and with higher resolution, this proportion may well increase. Five of these have three components (1221+18, 1423+24, 1623+26, 1628+36, 2325+26), two have four components (0814+22, 1058+11), and one source (2005−04) has a complicated structure but probably consists of four components (see the notes to Table 3).

For 0814+22 and 1058+11, the four components lie approximately on a straight line. In both cases the inner components are weaker than the outer components, and all four components have the same spectral index. In 0814+22, the inner components are larger than the outer components, whereas in 1058+11 all four components are about the same size.

For the "triple" sources, the central components is weaker at 2695 MHz than the outer components and appears to have a somewhat flatter spectrum. Also, the central component usually appears to be extended, although this result is a little uncertain due to signal to noise limitations. The source 2325+26 is an exception. There, the central component has a steep spectrum and is probably unresolved, and is considerably more powerful than the outer components. For three sources (1221+18, 1423+24, 2325+26), preliminary optical positions have been found by Hoskins (private communication), and in each case the central radio component coincides with the optical object.

VI. The "Largest Angular Size–Redshift" Plot

The correlation between the angular size and the redshift of extended quasars was first noticed by Miley (1968), and has been discussed further by Legg (1970) and Miley (1971). The relation is important for two reasons. First, it is one of the clearest relations that exists between any of the observable properties of quasars, and second, if the redshifts are assumed to be cosmological, it contains information concerning both the geometry of the universe and the evolution of quasars. (Although if evolutionary effects are large, geometrical effects are likely to be washed out.)

Miley (1971) noted the correlation between the "largest angular size" and the redshift for 127 quasars. (For sources consisting of more than one component, the "largest angular size" is taken to be the separation of the two outer components.) In Fig. 3 we show the same plot, with the 39 sources discussed in this paper added, bringing the total to 166 quasars. The new sources are shown as filled circles.

It is clear from Fig. 3 that the 39 new sources confirm the general trends observed previously. At any particular redshift there appears to be a rather well defined upper limit for the maximum angular extent attainable by an extended radio source. If the maximum linear sizes of these sources are assumed to be similar at different redshifts, then this suggests that their distances are at least an increasing function of their redshift.

Observations of radio galaxies and of quasars of small redshift indicate that the largest sources have linear sizes of about 500 kpc (assuming $H_0 = \text{km s}^{-1}\ \text{Mpc}^{-1}$). We have, therefore, drawn in Fig. 3 the expected relation between angular size and redshift for a source of linear size 500 kpc, for a static Euclidean world model (curve I) and for an Einstein-de Sitter model (curve II).

The relations are

$$\theta = 17.2/z \text{ arcsec} \qquad \text{(curve I)}$$

$$\theta = 8.6 \times \frac{(1+z)^2}{[1+z-(1+z)^{1/2}]} \text{ arcsec} \qquad \text{(curve II)}$$

Other Friedman models would give a relation slightly different from curve II, but the minimum in the angular size is due to the expansion of the universe as well as to space curvature, and occurs in all Friedman models. The limiting case is the Steady State model, for which the minimum angular size is approached assymptotically at infinite redshift, and would be 17.2 arcsec for the case considered here. The point of Fig. 3 is that the apparent upper limit in angular size seems to decrease as rapidly as $1/z$, and at redshifts greater than about 1.5 this differs significantly from the relation expected for a constant linear size in a typical Friedman model. It seems, therefore, that the linear extent of the largest quasars decreases rapidly with increasing redshift.

It is difficult to see how this effect could be due to selection. The angular data are complete above a few seconds of arc, and although these sources are from samples selected by flux density, there is no clear correlation between flux density and redshift. A selection effect of this kind could be caused by an anticorrelation between intrinsic luminosity and linear size. This would manifest itself as the sources lying well below the upper envelope in Fig. 3 having larger flux densities, and the sources lying close to the upper envelope having flux densities near the limit of the 4C survey (which includes over 70% of the sources in Fig. 3). Such an effect does not appear to exist, and so we conclude that the apparent decrease in the linear size of the largest quasars with increasing redshift is a real evolutionary effect.

An evolutionary effect of this sort is a natural consequence of radio source models that contain the radio components by the ram pressure of the intergalactic medium (De Young and Axford, 1967). As a component moves away from the parent optical object, it does work against the intergalactic medium. The distance at which it has expended its bulk kinetic energy and has come virtually to a standstill is, therefore, determined in part

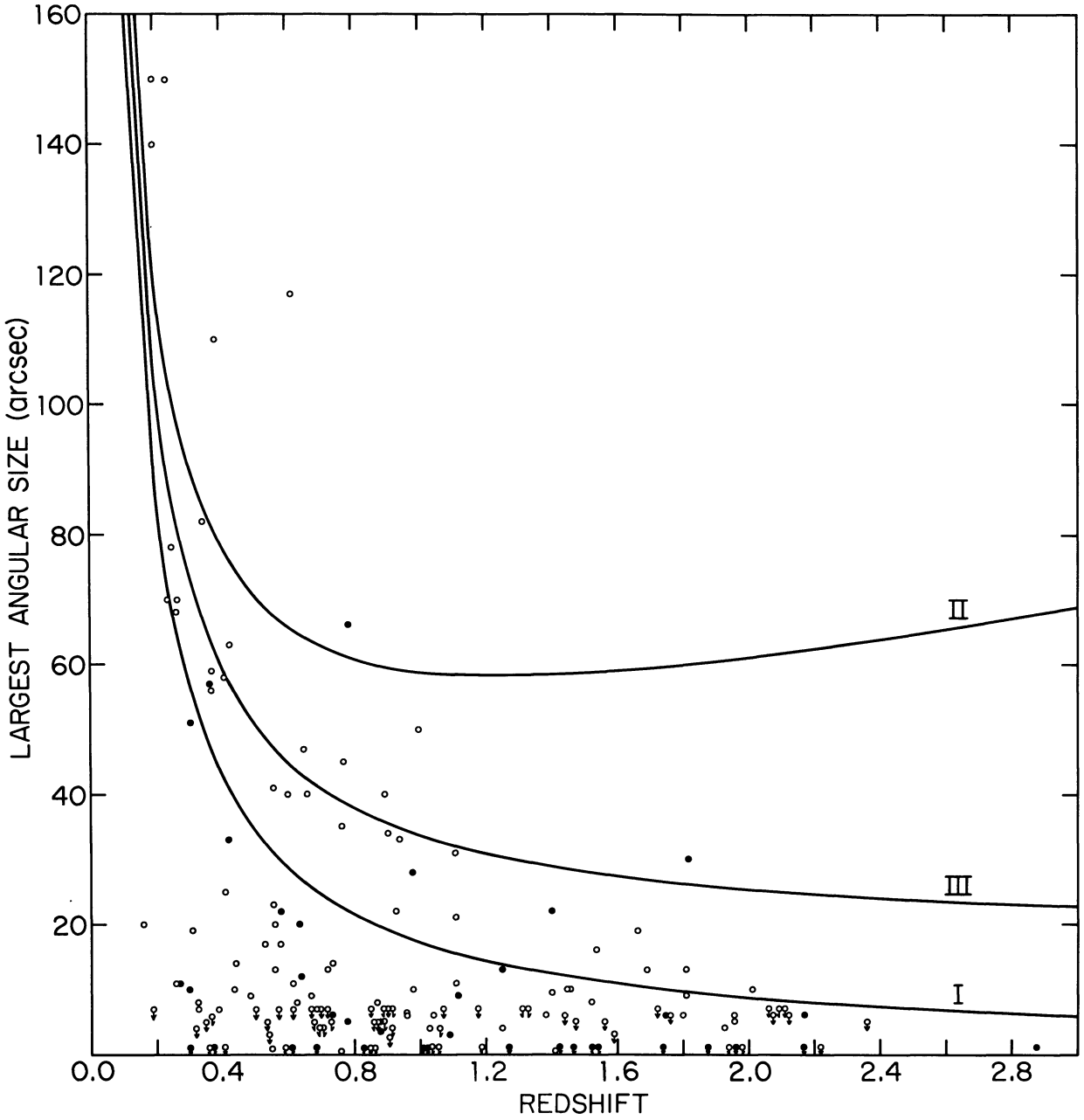

Fig. 3. "Largest angular size-redshift" plot for 166 quasars. The open circles are taken from the compilation by Miley (1971). The new sources discussed in this paper are shown as filled circles

by the density of the intergalactic medium. In all Friedman models, this density increases with redshift as $(1+z)^3$, and so we would expect that sources with similar initial conditions would attain smaller linear extents at larger redshifts. De Young (1971) has performed detailed numerical calculations on models of this type. Although the definition of a "stopping distance" is somewhat arbitrary; he finds that his results are described by a relation of the form

$$R_s(z) \sim R_s(0)\,(1+z)^{-4/5}$$

where R_s is the distance of the radio component from the parent object at the end of the rapid deceleration period, when the velocity is small. Incorporating this in an Einstein-de Sitter world model, the expected relation between angular size and redshift for $R_s(0) = 250$ kpc, is then

$$\theta = 8.6 \times \frac{(1+z)^{6/5}}{[1+z-(1+z)^{1/2}]} \text{ arcsec}.$$

This is shown as curve III in Fig. 3.

It is thus possible to account for a large part of the evolution in linear size in a very simple way. Other radio source models will give slightly different results. For example, in the simplified but analytic treatment

by Christiansen (1969), the "stopping distance" is proportional to $(1+z)^{-1}$. A similar result would be expected to hold for the model proposed by Rees (1971), since the evacuated "bubbles" in this theory are also prevented from expanding freely by the ram pressure of an external medium.

The scatter of points below the upper envelope in Fig. 3 may be due to a variety of causes. Projection effects are not very important, since only about 15% of the sources will have an apparent linear separation less than half their true separation. Some of the sources will be young objects that have not yet reached their full extent, but probably most of the scatter is due to scatter in the initial conditions (e.g. the momentum and internal energy of the components).

Because of the poor statistics at high redshifts, it is not clear whether the model described above accounts for all of the apparent evolution, or whether additional factors must be considered. Another way of producing similar evolutionary effects is to "snuff out" sources at high redshift before they reach their maximum extent (Rees and Setti, 1968). Christiansen (1969) derived an equation of motion for the radio components that can be written as

$$R(t) \sim 1.2\, R_s(1 - e^{-2t/t_s})$$

where the "stopping time" t_s is the time taken to reach R_s. If the source ceases to be visible after a time $t < t_s$, then the observed size of extended sources will be less than that expected from purely dynamical considerations. The radiative lifetime of a source may be limited by synchrotron or inverse Compton losses, or by escape of the relativistic particles by diffusion (De Young, 1970).

Inverse Compton losses against the universal microwave background are an attractive possibility since the losses increase rapidly at large redshifts. When these are combined with synchrotron losses, there exists a *maximum* lifetime for electrons radiating at a specific frequency. Van der Laan and Perola (1969) have shown that this occurs when the energy density of the magnetic field is one third of the energy density of the background radiation field. The corresponding lifetime is given by

$$t_r \sim 1.9 \times 10^9 (1+z)^{-3.5}\, \nu_0^{-1/2} \text{ years}$$

where ν_0 is the observing frequency in MHz. At frequencies above ν_0 the spectrum of the source falls off exponentially. However, none of the sources in Fig. 3 show such a break in their spectra up to 8085 MHz. For single burst models, we must conclude that their ages are less than $2.1 \times 10^7 (1+z)^{-3.5}$ years.

This leads to serious problems for the largest quasars at large redshifts. In Table 5 we give values of this lifetime at various redshifts. The third column gives the distance a radio component can travel in this time, if it is moving at the velocity of light. The fourth column gives the corresponding maximum angular separation of two such components traveling in opposite directions in an Einstein-de Sitter world model.

Table 5

z	$t_r(\nu_0 = 8085$ MHz) (10^5 years)	R_{max} (kpc)	θ_{max} (arcsec)
0	210	6400	∞
.5	51	1600	4500
1.0	19	580	136
1.5	8.5	260	61
2.0	4.5	140	34
2.5	2.6	80	21
3.0	1.6	49	13

Although no source in Fig. 3 actually violates the limits set in Table 5, many sources are within 10% of the limit. Almost certainly these limits are much too large. We have assumed that the break in the spectrum occurs just above 8085 MHz. In fact, if such a break exists, it probably occurs at much higher frequencies and θ_{max} is correspondingly reduced. Although the extended quasars in question have not been studied at very short wavelengths, it is interesting that Kellermann and Pauliny-Toth (1971) found no evidence for a high frequency cutoff in the spectra of other non-variable steep spectrum quasars, even at λ 3.5 mm. Secondly, it is improbable that the component velocity is near the velocity of light. Scheuer (1967) has argued that the near equality between the flux densities of the components of double radio sources implies that their velocity is almost certainly less than $c/3$. In detailed calculations of ram pressure models, De Young (1971) assumed an ejection velocity of $0.1\,c$, and the *average* velocity was $R_s/t_s \sim .02\,c$. If this is the case, then there is a serious conflict in the dynamic lifetimes implied by Fig. 3 and the radiative lifetimes in Table 5.

There are several ways to resolve the conflict. Of course, two obvious possibilities are that quasars are not at the distances indicated by their redshift, or that the microwave background radiation is not universal. A less radical explanation is that the simple "single burst" hypothesis is incorrect. Similar considerations concerning radiative lifetimes led van der Laan and Perola (1969) to reject such a model for producing the radio emission in radio galaxies. They proposed instead a model consisting of multiple non-cumulative bursts accompanied by rapid diffusion of particles from the radio emitting regions on a time scale shorter than the radiative lifetime of the electrons. But the foregoing discussion implies that some quasars are *older* than the radiative lifetime of the electrons. This suggests that *in situ* acceleration of electrons takes place, possibly associated with the compact objects envisaged by Burbidge (1967). It should be noted, however, as pointed out by van der Laan and Perola, that it may be difficult to reconcile such a model with the absence of very

steep spectra unless rapid escape of the radiating electrons by diffusion also occurs.

Acknowledgements. It is a pleasure to thank Drs. M. Schmidt and D. Wills for communicating redshifts in advance of publication, and Dr. D. Hoskins for measuring the optical positions. We are also grateful to Dr. E. B. Fomalont for use of his model fitting program, and to Drs. K. I. Kellermann and H. van der Laan for helpful discussions.

References

Burbidge, G.R. 1967, *Nature* **216**, 1287
Christiansen, W. 1969, *Monthly Notices Roy. Astron. Soc.* **145**, 327
De Young, D.S., Axford, W.I. 1967, *Nature* **216**, 129
De Young, D.S. 1970, *Astron. & Astrophys.* **9**, 125
De Young, D.S. 1971, *Astrophys. J.* **167**, 541
Fomalont, E.B. 1968, *Astrophys. J. Suppl.* **15**, 203
Greenstein, J.L., Oke, J.B. 1970, *Publ. Astron. Soc. Pacific* **82**, 898
Harris, D.E., Hardbeck, E.J. 1969, *Astrophys. J. Suppl.* **19**, 115
Hogböm, J. 1973, *Astron. & Astrophys.*, in press
Hogg, D.E. 1969, *Astrophys. J.* **155**, 1099
Hogg, D.E., Macdonald, G.H., Conway, R.G., Wade, C.M. 1969, *Astron. J.* **74**, 1206
Kellermann, K.I., Pauliny-Toth, I.I.K., Tyler, W.C. 1968, *Astron. J.* **73**, 298
Kellermann, K.I., Pauly-Toth, I.I.K. 1971, *Astrophys. Letters* **8**, 153
Kellermann, K.I., Jauncey, D.L., Cohen, M.H., Shaffer, D.B., Clark, B.G., Broderick, J., Ronang, B., Rydbeck, O.E.H., Matveyenko, L., Moiseyer, I., Vitkevitch, V.V., Cooper, B.F.C., Batchelor, R. 1971, *Astrophys. J.* **169**, 1
Laan, H. van der 1969, *Astron. & Astrophys.* **3**, 468
Laan, H. van der, Perola, G.C. 1969, *Astron. & Astrophys.* **3**, 477
Legg, T.H. 1970, *Nature* **226**, 65
Macdonald, G.H., Miley, G.K. 1971, *Astrophys. J.* **164**, 237
Mackay, C.D. 1971, *Monthly Notices Roy. Astron. Soc.* **154**, 209
Miley, G.K. 1968, *Nature* **218**, 933
Miley, G.K. 1971, *Monthly Notices Roy. Astron. Soc.* **152**, 477
Olsen, E.T. 1967, *Astron. J.* **72**, 738
Olsen, E.T. 1970, *Astron. J.* **75**, 764
Rees, M.J., Setti, G. 1968, *Nature* **219**, 127
Rees, M.J. 1971, *Nature* **229**, 312
Scheuer, P.A.G. 1967, in *Plasma Astrophysics*, Ed. P. A. Sturrock, Academic Press London
Wade, C.M. 1970, *Astrophys. J.* **162**, 381
Wardle, J.F.C., Miley, G.K. 1971, *Bull. Am. Astrophys. Soc.* **3**, 384
Wills, D., Lynds, R. 1970, *Nature* **226**, 532

J. F. C. Wardle
Department of Physics
Brandeis University
Waltham, Massachusetts 02154, USA

G. K. Miley
Sterrewacht
Leiden-2401, The Netherlands